Defense Technical Information Center Compilation Part Notice

ADP012073

TITLE: Oscillations of Ventilated Cavities Expermental Aspects

DISTRIBUTION: Approved for public release, distribution unlimited

This paper is part of the following report:

TITLE: Supercavitating Flows [les Ecoulements supercavitants]

To order the complete compilation report, use: ADA400728

The following component part numbers comprise the compilation report:
ADP012072 thru ADP012091

Oscillations of Ventilated Cavities Experimental Aspects

J.M. Michel
Laboratoire des Ecoulements Géophysiques et Industriels
BP 53 - 38041 Grenoble Cedex 9
France

1. Introduction

By injecting air in the low pressure regions of water flows, it is possible to obtain cavities similar to the attached cavities due to "true" cavitation. That ventilation is a current practice in the field of spillways for large concrete dams, especially in tropical zones. It is aimed to diminish the risks of erosion, as the speeds of the water flows ordinarily are very large : the stresses between concrete and water are diminished by the injected air, due to its compressibility which increases the characteristic time of contact and diminishes the forces for the same total impulse. Then the main problem is to calculate the ideal dimensions of the ducts by which atmospheric air is sucked up under the water flow (Chanson, 1999).

Here our main concern is rather on the side of ventilated hydrofoils or, possibly, torpedoes. In both cases, the main difference with respect to the case of vapour cavities is due to the non-condensable character of the gas which modifies the closure region of the cavities. For the latter case, the presence of gas inside the cavity can be produced either by the burning of powder for the body propulsion, or by the entrainment of atmospheric air at the body entry in water. Then initially there is a limited amount of gas inside of the cavity which progressively is shed into the cavity wake. On the contrary, hydrofoils are assumed to be supplied continuously with air, so that a steady regime is obtained, at least in the mean, which makes their study easier.

The concept of ventilated hydrofoil was imagined, about forty years ago, for the lift of rapid hydrofoil boats and even their propulsion by ventilated propellers. The shape of such a foil is shown on Figure 1 : it widens downstream as a parabola but can admit a small curvature.

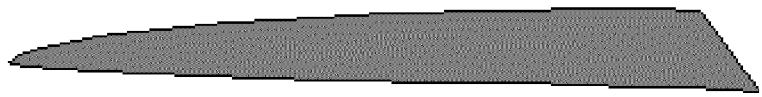

Fig. 1. Truncated foil with a ventilated base

The aft part of the foil is truncated, its upper side usually is shorter than its lower side. It is currently named "base-vented hydrofoil". Ventilation is operated artificially from an air compressor placed on the boat. Air passes by the legs of the boat or by the propeller hub and it is injected at the base of the foils or the propeller blades : the pressure at the base of the foil is increased and the drag is lowered. If the angle of attack becomes important, air tends to invade the region of the flow close to the foil upper side, which results in the decrease of the lift. That flow regime must be avoided, and then the possible range of incidences currently is rather small.

This kind of foil seems to be well enough suited to boat speeds in the range 40-80 knots, for which classical, non-cavitating foils are inoperative. For larger speeds, only supercavitating foils with a non

Paper presented at the RTO AVT Lecture Series on "Supercavitating Flows", held at the von Kármán Institute (VKI) in Brussels, Belgium, 12-16 February 2001, and published in RTO EN-010.

wetted upper side can be used (as for example in pump inducers of cryogenic liquids used in rocket propulsion).

For base-vented hydrofoils with wetted upperside, several problems have to be considered (*Rowe* 1979). Firstly, the global operation of the foil is characterized by the dependence of the cavity length, the lift and drag coefficients on the foil geometry and the relative underpressure of the cavity σ_c (cf chapter 1, § 1.4.3) :

$$\sigma_c = \frac{p_r - p_c}{\frac{1}{2}\rho V^2} \quad \textbf{(1)}$$

Here p_r stands for the reference pressure upstream of the foil and p_c for the cavity pressure, the latter being the sum of the vapour pressure (as it can be assumed that the cavity is saturated in vapour) and the mean pressure of the injected air :

$$p_c = p_v + p_{air} \quad \textbf{(2)}$$

Secondly, we need to know the limits of operation corresponding to cavitation inception near the leading edge or to the venting of the foil upper side. As the radius of curvature at leading edge of such foils usually is very small, the first limit is the strictest one, which justly leads to small possible ranges of incidence.

Finally, in the expression (2) for p_c and then for σ_c, the contribution of p_{air} is not known when the air flowrate is imposed : the balance of pressures depends on the mode by which air is evacuated at the rear of the cavity. The evacuating mode depends on the global flow geometry, particularly the length of the cavity and the circulation, so that all parameters are in mutual dependance. An additional difficulty comes from the fact that several air evacuation regimes are possible, even for a cavity confined at the base of the foil. Thus the non-condensable character of air makes the behaviour of ventilated cavities deeply different from the vapour cavities.

2. Non-Dimensional Parameters

By analysing the experimental results (Michel 1971, 1984) it appears that it is necessary to distinguish two terms in the relative underpressure σ_c, such as $\sigma_c = \sigma_v - \sigma_a$:

- the classical parameter cavitation σ_v, which characterizes the ambient pressure :

$$\sigma_v = \frac{p_r - p_v}{\frac{1}{2}\rho V^2} \quad \textbf{(3)}$$

- the relative mean pressure of air inside the cavity, which takes the elastic behaviour of air into account :

$$\sigma_a = \frac{p_{air}}{\frac{1}{2}\rho V^2} \quad \textbf{(4)}$$

Note that, as σ_c is usually small, the parameters σ_v and σ_a are not very different.

In the case of *pulsating ventilated cavities*, we have also to consider the ratio σ_c/σ_a which compares the cavity underpressure to the mean pressure of air (or, in an almost equivalent way, the parameter σ_c/σ_v, as done by *Silberman* and *al*, 1961, and *Song* (1962), who described the pulsating regime for the first time).

In this case also, if f, ℓ and d stand for the pulsation frequency, the mean cavity length and a fixed reference length respectively (*e.g.* the chord of the forebody for the latter), the phenomena are well enough described when we introduce the non- dimensional frequency :

$$\varphi = \frac{f}{\sqrt{\frac{p_{air}}{\rho d \ell}}} \tag{5}$$

Finally, considering the mass air flowrate Q_m and a reference area S, we can build the following non-dimensional parameters :

• the mass air flowrate coefficient :

$$C_{Qm} = Q_m / \rho V S \tag{6}$$

• the volume air flowrate coefficient :

$$C_{Qv} = Q_m / \rho_{air} V S \tag{7}$$

The mean air density ρ_{air} is known through the measurement of the cavity pressure p_c and the use of the Boyle-Mariotte law. If we consider the mean velocity V_{air} of air inside the cavity and take an area close to the cavity cross-section for S, we have, approximately : $Q_m \cong \rho_{air} V_{air} S$, so that the volume airflow coefficient C_{Qv} more or less represents the ratio of the air velocity to the water velocity : V_{air}/V. Practically, the values of C_{Qv} can be markedly lower than 0.1, and they can also reach values of the order 0.7 to 1.

Of course, other classical non-dimensional parameters must be considered, and among them especially the Froude number $V/\sqrt{gd}$.

3. Experimental Results

3.1. DEPENDENCE BETWEEN NON-DIMENSIONAL PARAMETERS

Experimental tests operated in various configurations (two or three-dimensional wings, cavity formed between an horizontal water jet and a solid wall, free surface channel or closed channel...), bring three main dependences in light (in all those relations, the main influence parameter is in bold type characters) :

- The relative mean cavity length ℓ/d and the global force coefficients depend on the foil incidence, the Froude number and the relative cavity underpressure :

$$\frac{\ell}{d}[\alpha, Fr, \boldsymbol{\sigma_c}] \tag{8}$$

- The relative air pressure σ_a depends on the incidence, the mean ambient pressure and the mass air flowrate coefficient :

$$\sigma_a[\alpha, \sigma_v, \boldsymbol{C_{Qm}}] \tag{9}$$

Note that from the experimental point of view, a more convenient way to express that dependence is :

$$C_{Qv}[\alpha, \sigma_v, \boldsymbol{\sigma_c}] \tag{10}$$

- The non-dimensional frequency φ depends particularly on the ratio σ_c/σ_a :

$$\varphi\left[\frac{\sigma_c}{\sigma_a}\right] \tag{11}$$

Some experimental results which illustrate those relations are presented below. Most of them were obtained with a two-dimensional flow realized in a rectangular, free-surface channel (width 175 mm, height 280 mm). The fore-body was a simple triangular wedge (chord c = 60.5 mm, base b = 17 mm) placed at at a zero mean incidence and different submersion depths : h_1 = 70, 140 or 210 mm. The water velocity V could be varied between 2 and 14 m/s, while the absolute pressure p_0 over the free surface was fixed between a value close to the water vapour pressure and the atmospheric pressure. Then the range of actual values for the cavitation number σ_V was between 0.04 and 20 approximately. It is valuable to note that the hydrodynamic tunnel in which such experiments are carried out must be able to eliminate the large amounts of the injected air so that the water entering the test section be free from all trace of air after recirculation in the tunnel loop.

3.2. RELATIVE CAVITY LENGTH ℓ/C AS A FUNCTION OF σ_C

In Fig. 2, the main dependence of the relation (8) is shown for four values of the velocity V and an immersion depth h = 140 mm. Note that the experimental points correspond to various values of the cavitation number σ_v, between 0.4 and 10 approximately. Thus the influence of the ambient pressure on the different air flow regimes does not appear on such a graph.

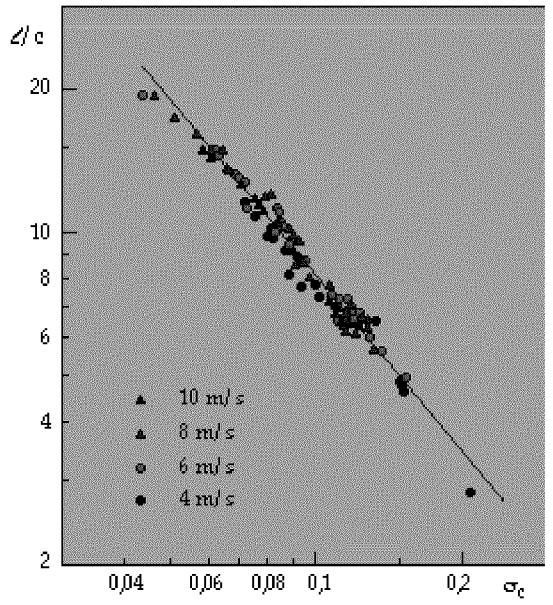

Fig. 2. Variation of the mean non-dimensional length of the cavity versus the relative underpressure σ_c

Considering the almost linear dependence of ℓ/c *vs.* σ_c in logaritmic coordinates, we can adopt a power law : $\ell/c = A\ \sigma_c^{-n}$. The following table gives the values of A and n for the three values of the submersion depth :

h(mm)	A	n	Variations of ℓ/c
70	0.38	1.16	3.4-23
140	0.45	1.26	2.8-19
210	0.34	1.47	3.6-21

Those values are close to the ones corresponding to vapour supercavities. The theoretical asymptotic value of n in an infinite medium is 2 (for small σ_c), while a simple model considering the flow above the wedge and the cavity as a simple jet gives the value n = 1.

The Froude number has a small influence on the cavity length, at least for the present range of velocities and chord length, except for the smallest values of σ_c. In fact, if we consider the Froude number based on the cavity length, we obtain the small value $Fr_\ell = 2.4$ for ℓ/c = 18 (or ℓ = 1.09 m) and V = 8 m/s. which makes likely the gravity effect, as seen on the Figure 2.

3.3. AIR FLOW RATE

The sketch of Figure 3 represents the relation (10), together with the flow behaviour, when the air flowrate is gradually increased then decreased between small and large values. Here we suppose that σ_v is large enough so that there does not exist any vapour cavity before the air injection.

Remark : If such a cavity is present, the initial value of σ_c is equal to σ_v, and the phenomena are practically as in Figure 3. However, for very small values of σ_v, say lower than about 0.2, it was found that a very small amount of air results in a sudden, and large, increase of the cavity length, disclosing a kind of global flow instability. We don't consider that case here.

Roughly speaking, the curve of Figure 3 is L-shaped. For the very small air flowrates, the air escapes downstream of the cavity as separate bubbles which are later entrapped in the alternate Benard-Karman vortices of the body wake. For larger air flowrates, a continuous air cavity appears and it is possible to consider and measure the parameter σ_c (the initial point on the right hand of Figure 3). A subsequent small increase of Q_m produces large variations in the air pressure, the σ_c - value and the length of the cavity : that is due to the difficulty, for air, to escape from the cavity (see below). On the contrary, on the vertical branch of the curve, air is evacuated by big separated bubbles. Those bubbles can leave the cavity upstream of its termination, under the gravity effect. That mode of air evacuation is very efficient, so that usually the parameter σ_c tends to a positive minimum value σ_m (and the cavity length to a maximum value). Subsequent tests (*Laali* and al 1984, see below) gave values between 0.01 and 0.09 for the parameter σ_m. It decreases when the Froude number increases and it depends also on the ambient air pressure *via* the parameter σ_v.

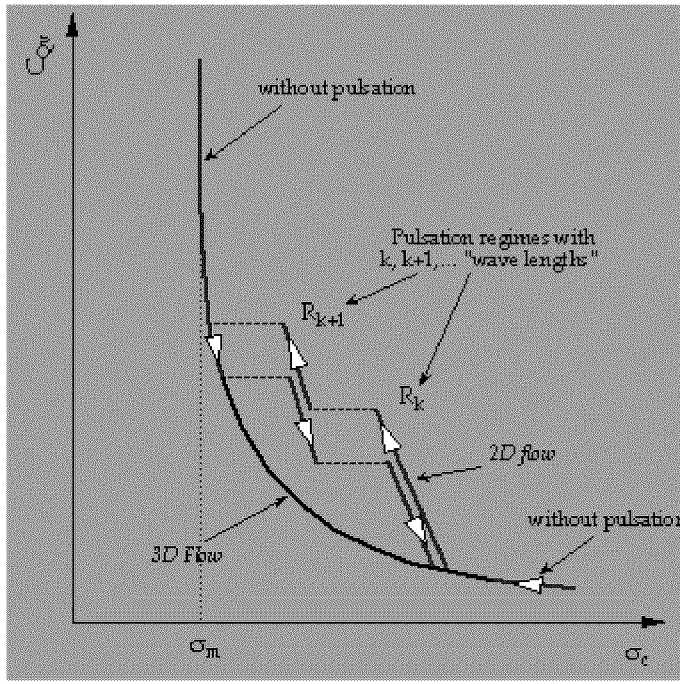

Fig. 3. Typical evolution of the cavity for an increasing, then decreasing, air flow rate (σ_v is constant)

3.4. PULSATING REGIME

In two-dimensional flows, the connecting region between the horizontal and vertical branches of the curve of Figure 3 is characterized by periodic pulsations of the air cavity : undulations are convected, with an increasing amplitude, on both free frontiers. They join at the rear part of the cavity, thus allowing air to escape under the form of separate, periodic, air pockets, as shown on Figure 4 (that figure sketches experimental results which were obtained through a special device for a one wave cavity (*Michel*, 1971). Then the air pressure undergoes periodic, almost sinusoidal, fluctuations. Their minimum occurs at the instants when the air pockets leave the cavity. At the same instants, undulations of the free surfaces, pointed to the cavity interior, arise at the two trailing edges of the wedge. And then the cavity, which passes by its minimum length, has the shape of one or several spindles : the corresponding flow regimes are named R_1, R_2, ..., R_k (Regime R_2 is presented in Figure 4). In general, the largest values of k are obtained for large values of the ambient pressure or, more precisely, for the small values of the parameter σ_c/σ_a.

When the regime R_k is established, a small increase in the ventilation air flowrate can result in the passage to the regime R_{k+1}, as shown in Figure 3. That occurs for threshold values of the parameter C_{Qv}. For decreasing values of the airflow, the passage from regime R_{k+1} to R_k occurs for lower values of C_{Qv}, so that the total evolution of the ventilated cavity exhibits a hysteretic aspect. As indicated on Figure 4, the wake of the cavity is featured by separate, almost periodical, air pockets, which have been emitted during the previous periods.

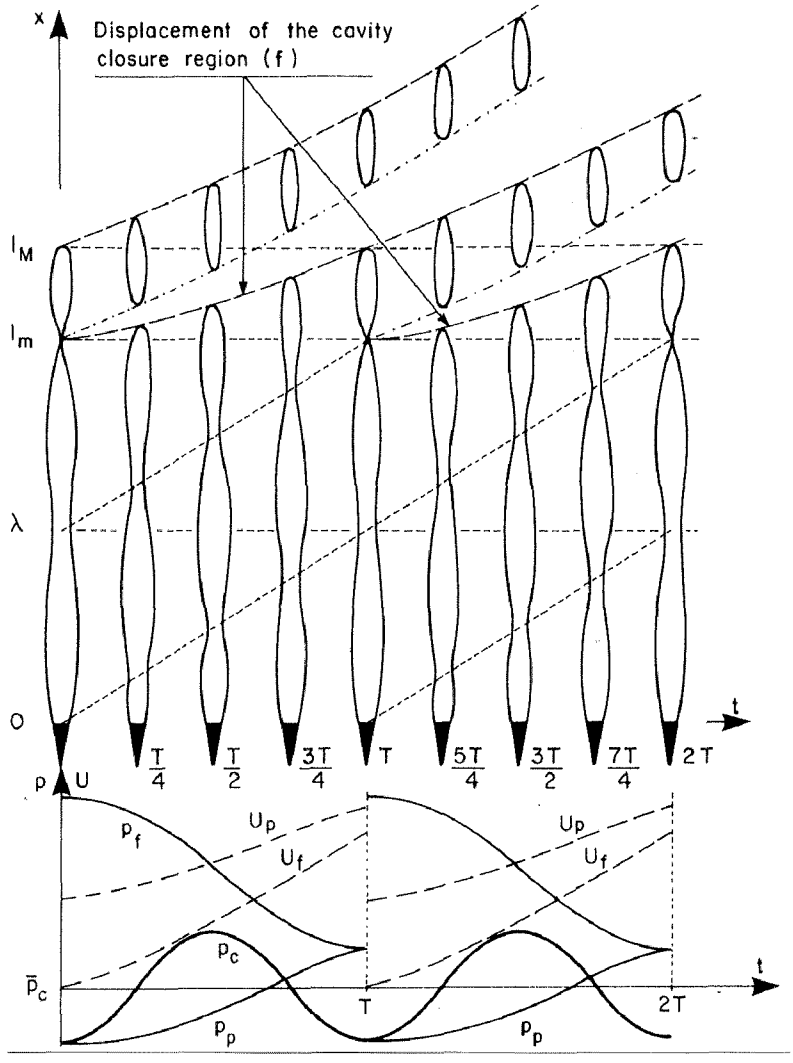

Fig. 4 A schematic view of the evolution of a two-waves cavity over two periods

- For comparison, the above mentioned *Laali* tests (*Laali et al* 1984) were carried out with the so-called "half-cavity" configuration, *i.e.* the cavity formed between an initially horizontal plane water jet, the thickness of which was H, and a solid plate having a small slope β. The distance between the jet and the plate is named h (see the Figure 5).

  Note that here the reference pressure p_r in the definition of σ_c and σ_v is the pressure p_0 above the jet. That configuration is a possible model for the spillway aerated flow mentioned in the Introduction to the present Chapter. The main features of the ventilated cavities downstream bodies were present also in that case : trends of the relations $\ell(\sigma_c)$ and $C_{Qv}(\sigma_c)$, pulsating regimes, relation $\varphi(\sigma_c/\sigma_a)$... In particular :

  a. The dependence between the cavity length ℓ and the relative cavity underpressure σ_c takes the approximate form :

$$\ell \cong \frac{4}{3}\sqrt{\frac{Hh}{\sigma_c}}\left[1+\sqrt{\frac{Hh}{\sigma_c}}\sin\beta\right]$$

b. The threshold value of the volume flowrate coefficient C_{Qv} for the passage of the regime R_1 to the regime R_2 diminishes when the parameter σ_v increases, either by the growing reference pressure p_0 or by the decreasing jet velocity V.

c. The dependence $C_{Qv}(\sigma_c)$ is practically not influenced by the step height h, neither as regards the threshold values of C_{Qv} nor the jumps in the σ_c-values. The maximum value of the jump occurs in the regime R_1 and is of the order 0.01-0.02.

d. Finally, the minimum value σ_m of σ_c seems to be controlled by the transverse pressure gradient inside the water jet, which influences the rising of the air bubbles for the high rates of ventilation.

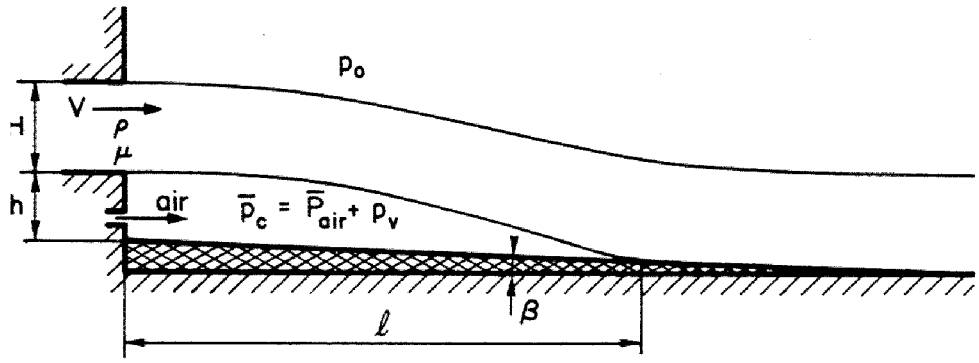

Fig. 5 Sketch of the half-cavity flow

Returning now to the case of the cavities behind the wedge, it is observed that, if the gravity effect is negligible, the air pockets tend initially to be symmetrical with respect to the flow direction. However, further investigations have shown that subsequently air is not present as a continuous medium in the air pocket, rather as small bubbles organized in alternate vortices. When the Froude number is small (for small water velocities), the air pockets are no longer symmetrical and the wake of the cavity looks a "duck file" : that seems to be due to the deviation of the reentrant jet from the axial direction under the gravity effect (see the Figure 6).

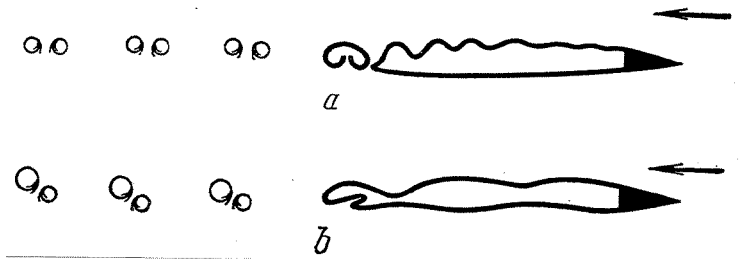

Fig. 6 Influence of gravity on the reentrant jet direction and the arrangement of the vortices in the wake.

3.5. THE AIR BLOCKAGE CONDITION FOR PULSATION

The basic reason for the discontinuous release of air at the rear part of a ventilated cavity is to be looked for in its geometry : since cavity is an underpressure region, the curvature of its frontiers tends to be directed towards its interior so that - in steady, 2D or axisymmetric flow - those surfaces tend to join themselves and to produce a reentrant jet which prevents the outflow of air. That *blockage condition* can be illustrated in an experimental way : if we put two parallel plates downstream a ventilated, pulsating,

cavity (see Figure 7), the curvature of the frontiers is locally reversed and air can flow in a continuous way. Then the pulsations disappear and the global flow becomes steady.

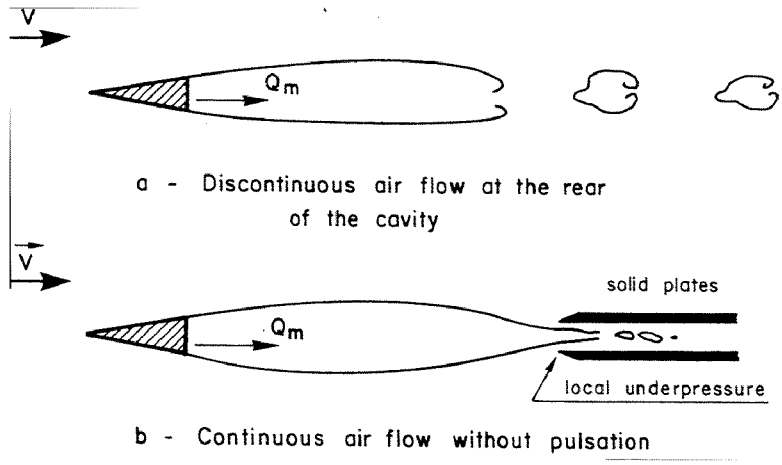

Fig. 7.

Another way for the air escape can be observed in the case of a ventilated three-dimensional hydrofoil with a small aspect ratio : a part of the injected air is evacuated continuously through the tip vortex, which tends to weaken, or even to suppress, pulsations (*Verron*, 1977), and *Verron* and al (1984). A similar observation was made by *Cox et al* (1957) for the horizontal ventilated cavity behind a vertical disk, at low Froude number. In this case the cavity ended by two almost parallel vortices by which air was evacuated into the wake. A physical model taking the gravity in account allowed the authors to give an account of the main flow features, ie the distance between the vortices, their diameter and the air flowrate.

Now, in the case when pulsations do exist, their periodical character results from a phase synchronization between the production of the undulations near the forebody and their coming to the rear part of the cavity (as suggested in Figure 4). Air pressure plays an important role in that mechanism as it conveys information from the rear to the fore part of the cavity (see below).

3.6. PULSATION FREQUENCY

Roughly speaking, the frequency of pulsations varies as $\sqrt{P_{air}}$ in each regime R_k. That result appears in Figure 8 for regime R_1. It leads us to build the non-dimensional frequency φ as defined by relation (5) and study its variation versus the parameter σ_c/σ_a (Figure 9).

It is noticeable that the various pulsating regimes are determined by ranges of σ_c/σ_a. values. In particular, the one-wave regime corresponds to the range 0.06 - 0.25 of that parameter, as well for a closed channel that a free surface channel. Also, higher the rank of the regime, narrower the range of σ_c/σ_a. In each regime, the dependence $\varphi(\sigma_c/\sigma_a)$ is roughly linear. The total variations of φ are between about 0.7 and 1, *i.e.* a small enough range (the limits are slightly smaller in the case of a deeper submersion of the forebody). It follows that the pulsation frequency is roughly proportional to the inverse of the mean length of the cavity.

In case of lifting foils, the circulation around the cavity can also influence the mode of air evacuation at its rear part, as indicated by relations (8) and (10). Then it happens (*Michel* 1984), that under only slight variations of the angle of attack α, (all other parameters being kept constant, in particular σ_v and the mass airflow rate Q_m) , the lift and drag coefficients may change : variations of α may result in a change of regime and then of σ_c.

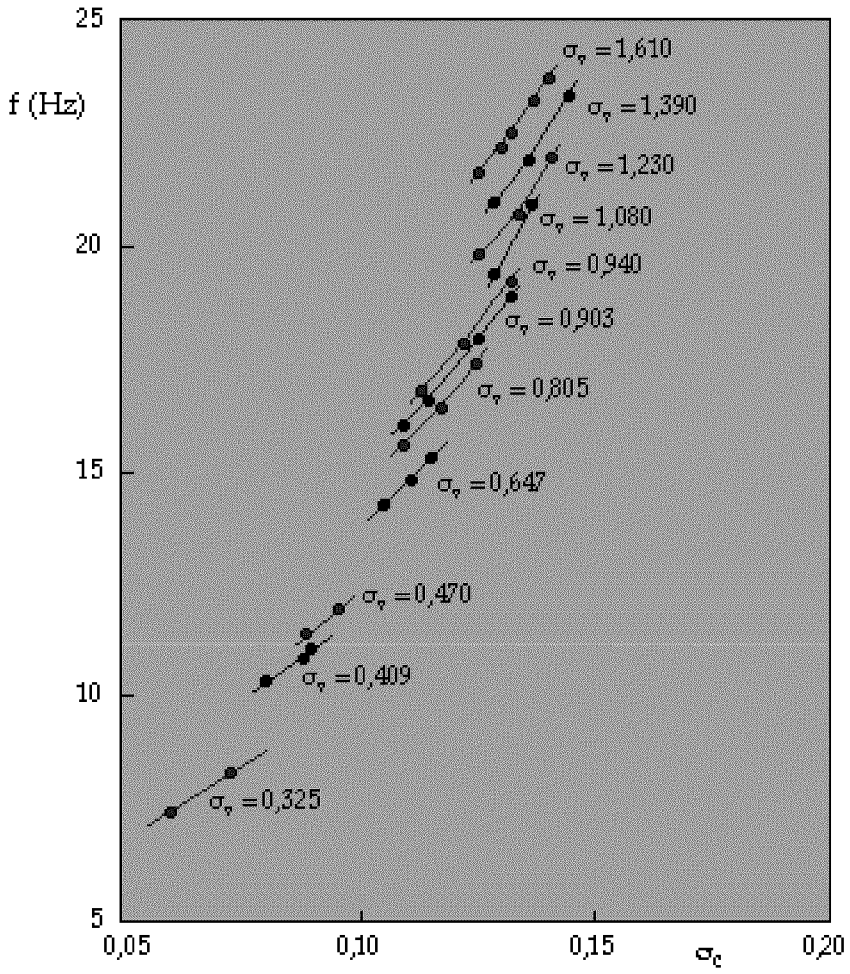

Fig. 8. Variations of the frequency f vs σ_c for increasing values of σ_v (Regime R_1, h_1 = 21 cm, V = 8 m/s)

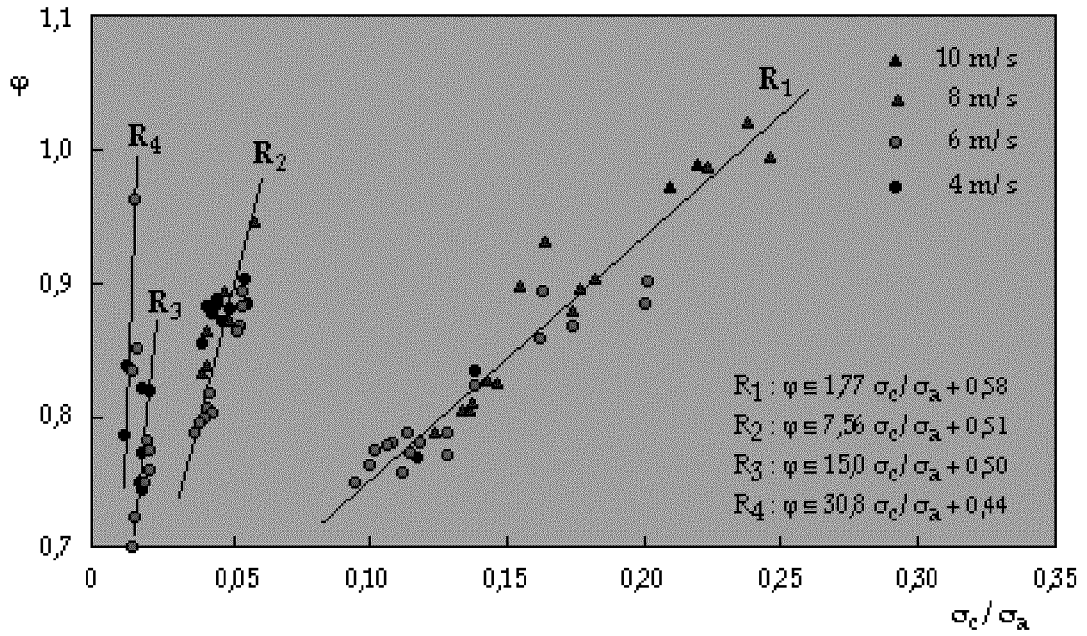

Fig. 9. Non-dimensional frequency vs. σ_c/σ_a (h_1 = 7 cm)

4. On the Pulsation Mechanism

As suggested in the Figure 4, different parameters can be described, as connected to the evolution of a ventilated, pulsating, cavity.

- For the experimental conditions in view, the existence of pressure waves inside the cavity cannot be considered and the pressure p_c is uniform through the cavity. The measurement of p_c shows that it fluctuates practically as a sinusoidal function of time, at the frequency f. Its minimum value corresponds to the instant at which an air pocket is shed in the wake of the cavity.
- The length λ, $\lambda = V_c/f$, where V_c stands for the mean velocity of water at the cavity frontier, *i.e.* $V_c = V\,(1 + \sigma_c)^{1/2}$, can be considered as a wave length for the cavity pulsation. In a regime R_k, it is connected to the minimum cavity length ℓ_m by the relation :

$$\ell_m = k\lambda \qquad \textbf{(12)}$$

- That relation agrees with the above-mentioned phase relation between the birth of the fluctuations of the free surfaces near the wedge trailing edges and the instant of the shedding of the air pocket.
- The overpressure p_f, which is created in the closure region at the instant of the juncture between both cavity interfaces, diminishes when the air pocket moves away from the cavity with the velocity U_p.
- The pressure p_p in the air pocket, which initially is equal to p_c, grows subsequently until the p_f-value. Then the volume v_p of the pocket decreases while it is accelerated inside the cavity wake.
- The velocity U_f of the rear of the cavity is initially zero and then grows until the velocity-value of the air pocket.

That simple examination shows that all parameters undergo mutually consistent variations. In order to complete the description, we have to invoke several specific relations :

- The air mass in the air pocket is Q_m/f.
- The velocities U_f and U_p are related to the variations of the cavity volume v_c and the virtual mass of the air pocket.
- The variations of v_c result from the perturbations of the transverse velocity v at the interfaces.
- They are connected to the flow rate Q_m by the relation :

$$\frac{d(p_c v_c)}{dt} = Q_m \times \text{constant}$$

- A special condition can be used, as was done by *Woods* (1964,1966), in order to avoid the pressure singularity at infinity in a 2D field of flow : to cancel the variations of the total volume "cavity plus cavity wake". That condition means that energy exchanges between the cavity and its wake have to be considered. Here, it could be approximated by the condition that the variations of the cavity volume are balanced by the volume variations of the first air pocket in the wake.

The Wood's condition meets the experimental observation of pulsating cavities in free surfaces channels : in most of the cases, the free surface is not affected by the pulsations, which suggests that the exchanges are mainly in the streamwise direction, not in the transverse one. It allows understanding that pulsating cavities can be produced in closed channels and in the configuration of the half-cavity, as described by *Laali et al* (1984). Let us note that, for the reduced pulsation ω_k defined by the expression :

$$\omega_k = \frac{\pi f \ell_m}{V_c} = \frac{\pi f \ell_m}{V\sqrt{1+\sigma_c}}$$

Woods gets the theoretical relation :

$$\omega_k = 1.97 + \pi\,(k-1)$$

while the experimental relation (12) can be rewritten as :

$$\omega_k = \pi k.$$

4. Final Remark

The behaviour of ventilated cavities, namely their stability and the pulsating regimes, was theoretically studied in the case of 3D axisymmetrical flows by Parishev (1978), who used several simplifications previously proposed by Serebryakov (1973) and Logvinovich (1976). More recently, Semenenko (1998) and Semenov (1998) proposed theoretical descriptions of the pulsating regimes in the case of 2D, plane flows.

References

CHANSON, H. -1999- The Hydraulics of open channel flow - An Introduction. *Butterworth-Heineman Publishers*. Oxford (England). 544 p.

COX, R.N. & CLAYDEN, W.A. -19575- Air entrainment at the rear of a steady cavity.*Symp. on Cavitation in Hydrodynamics.* NPL, Teddington (England)

LOGVINOVICH, G.V. -1976- Problems of the theory of axixymmetrical cavities. *Tsagi*, **1797.**

LAALI, A.R. & MICHEL, J.M. -1984- Air entrainment in ventilated cavities : case of the fully developed "half-cavity" *J. of Fluids Engineering*; **106, 3**, 327-335.

MICHEL, J.M. -1971- Ventilated cavities : a contribution to the study of pulsation mechanism. *Symposium IUTAM on rapid, non steady liquid flows*, Leningrad.

MICHEL, J.M. -1984- Some features of water flows with ventilated cavities. *J. of Fluids Engineering*; **106, 3**, 319-326.

PARISHEV, E.V. -1978- Theoretical study of the stability and pulsations of axisymmetric cavities. *Tsagi.*

ROWE, A. -1979- Evaluation of a three-speed hydrofoil with wetted upper side. *J. of Ship Research*, **23, 1**, 55-65.

SEMENENKO, V.N. - 1998- Instability and oscillation of gas-filled supercavities. *3rd International Symposium on Cavitation*, Grenoble (France), Proc., Vol 2, 25-30.

SEMENOV, Y.A. - 1998- Exact solution of problem of unsteady cavitation flow past wedge. *3rd International Symposium on Cavitation*, Grenoble (France), Proc., Vol 2, 55-59.

SEREBRYAKOV, V. -1973- Asymptotic solution of the problem of slender axisymmetric cavity. *Reports of the NAS of Ukrainia,* **A 12**, 1119-1122.

SILBERMAN, E. & SONG, C.S. -1961- Instability of ventilated cavities. *J. of Ship Research*. **5, 1**, 13-33.

SONG, C.S. -1962- Pulsation of ventilated cavities. *J. of Ship Research*, **5, 4**, 1-20.

VERRON, J. -1977- Écoulements cavitants autour d'ailes d'envergure finie en présence d'une surface libre. *J. de Mécanique*. **12, 4**, 745-774.

VERRON, J. & MICHEL, J.M. -1984- Base-vented hydrofoils of finite span under a free surface : an experimental investigation. *J. of Ship Research*. **28, 2**, 90-106.

WOODS, L.C. –1964- On the theory of growing cavities behind hydrofoils. *J. Fluid Mech.*, **19-1**, 124-136.

WOODS, L.C. –1966- On the instability of ventilated cavities. *J. Fluid Mech.*, **26-3**, 437-457.